scientific reports

OPEN

Characterization and evaluation of Fe^{2+} and Mn^{2+} in reservoirs and sediments in the Jianghuai Region

Kun Wang, Wei Chen, Yuchao Tang, Beiping Zhang, Haixiang Sun, Changnian Wu, Jian Huang & Xianhuai Huang✉

A dynamic monitoring study of water quality and sediment was conducted in August 2024 at four drinking water reservoirs in Hefei City (Dafangying, Dongpu, Modun, and Zhongxing Reservoirs). Monitoring results indicate: (1) Compared to the summer of 2018, overall Fe and Mn levels in Hefei's reservoirs showed improvement during the summer of 2024. Excessive Fe and Mn concentrations were only observed at deeper water levels, with no exceedances detected in surface layers. (2) Vertical monitoring analysis revealed that due to high summer temperatures, a thermocline formed at approximately 8 m in all four reservoirs. At this depth, the temperature difference between the surface and bottom layers was about 7 °C, resulting in a positive correlation between T, DO, TP, Fe, and Mn. (3) Monitoring of vertical distribution of Fe and Mn in reservoir sediments indicates overall surface enrichment characteristics, with highest concentrations in the surface layer decreasing gradually with sediment depth. (4) Morphological analysis of Fe and Mn in surface sediments indicates that Fe primarily exists as a residual form, while Mn predominantly occurs in a reducible state.

Reservoir-type water sources are important sources for urban water supply, and the water quality directly affects the safety of urban drinking water[1]. Both Fe (iron) and Mn (manganese) are typical redox-sensitive elements, especially in summer when the water is deep and prone to thermal stratification, easily allowing the release of these elements from the sediment into the overlying water under reducing conditions. When their concentrations exceed certain standards, various negative effects can occur. For example, the pollution can affect the sensory characteristics of the water. High concentrations of Fe may cause the water to appear reddish-brown or turbid, increasing turbidity and affecting the taste and odor of the water. One major cause of water quality pollution is the release of compounds from the surface sediment into the water system, known as internal pollution. For reservoirs with high eutrophication levels, the bottom water is seasonally anaerobic, leading to serious periodic internal pollution from sediment[2].

Sediments are the primary accumulation site for pollutants in reservoirs[3,4], and the heavy metals enriched in these sediments have received widespread attention due to their ability to accumulate, resist degradation, and pose significant harm[5–7]. Pollutants in the sediment can, under certain conditions, be released into the water through diffusion, convection, or resuspension, causing secondary pollution[8]. Survey results indicate that large and medium-sized lakes (such as China's Dianchi Lake[9], Chaohu Lake[10,11], and the Great Lakes in the United States[12,13]) have severe eutrophication problems, with internal pollution being the leading factor in seasonal water quality degradation. For example, in a Swedish lake, 99% of the nutrients in the summer come from internal pollution of the sediment[14]. For shallow lakes with high organic content in the sediment, internal release is also an important factor influencing organic pollution in the water. Numerous studies have proven that microbes, under anaerobic conditions, can use high-valence metals in the sediment as electron acceptors to anaerobically decompose organic matter[15].

Through continuous field monitoring of Dafangying Reservoir in 2018, methods such as Pearson correlation analysis were employed to clarify the relationship between dissolved oxygen and water quality. Results indicate that dissolved oxygen concentrations in the reservoir are higher during spring and winter, lower in summer and autumn, with significant seasonal fluctuations occurring in autumn. Once stable thermal stratification formed, seasonal hypoxia or even anoxia occurred in the bottom water layer. Thermal stratification was a key driver of vertical dissolved oxygen concentration variations and manganese concentration differences, particularly in the bottom layer[16]. Particularly in summer, Mn concentrations in bottom waters reached several times those in

surface waters. During summer and early autumn, bottom water Mn concentrations severely exceeded standards, peaking at 0.9 mg/L. Concurrently, manganese concentrations in the reservoir's pore water reached as high as 17.49 mg/L. During winter, the water body maintains vertical homogeneity with sufficient dissolved oxygen at all monitoring points. Mn^{2+} concentrations reach their annual minimum, and no Mn exceedances occur. Mn in sediments readily releases manganese ions, influenced by water quality and pH; pH variations significantly affect manganese release, while calcium ions also promote Mn release from sediments. Building upon prior research, this study incorporates additional monitoring data from three reservoirs and analyzes relevant data on iron (Fe), manganese (Mn), and other ions in the water and sediments of four Hefei reservoirs (Dongpu Reservoir, Dafangying Reservoir, Zhongxing Reservoir, Modun Reservoir) during the summer flood season of 2024. A preliminary risk assessment is conducted based on the analysis of the detection data. This ongoing systematic analysis of pollution characteristics and trends in water bodies and sediments across reservoirs aims to provide early warnings for potential future Fe and Mn pollution issues, offering new insights for reservoir Fe and Mn pollution prevention and control, as well as regional drinking water safety assurance.

Material and methods
The study area
Hefei City is located in the central part of Anhui Province, China, and is a city with abundant water resources. The city has numerous reservoirs, many of which hold significant ecological and environmental value. This study analyzes four of the larger drinking water reservoirs in Hefei, namely Dafangying Reservoir (with a total storage capacity of about 316 million cubic meters and a water surface area of approximately 6.7 square kilometers), Dongpu Reservoir (with a total storage capacity of about 150 million cubic meters and a water surface area of approximately 5.2 square kilometers), Zhongxing Reservoir (with a total storage capacity of about 130 million cubic meters and a water surface area of approximately 4.5 square kilometers), and Modun Reservoir (with a total storage capacity of about 100 million cubic meters and a water surface area of approximately 3.5 square kilometers). Considering that water flow characteristics can affect the distribution of Fe and Mn, especially in slower-flowing areas where Fe and Mn may accumulate more, and the phenomenon of stratification in reservoirs is more common in the summer, different water layers may have different Fe and Mn concentrations. Sampling points were set at the upstream, downstream, center, and shore of each reservoir, and both water and sediment samples were collected. The specific sampling locations are shown in Fig. 1 (The satellite image is from the Earth Star Map 2024, URL: https://online.geovisearth.com). The latitude and longitude of the sampling points are shown in Table 1.

Sampling and analytical methods
Water samples were collected using a 1000-ml acrylic sampler and stored in 500-ml polyvinyl chloride bottles. On-site measurements included temperature, dissolved oxygen (Hach HQ40d-, Hach Analytical Instruments (Shanghai) Co., Ltd.), conductivity (Bante530-s, Hangzhou Bante Instruments Co., Ltd.), pH, and ORP (DZB-718L, Shanghai Leizhi Instruments Co., Ltd.). Separate water samples were filtered through 0.45 μm syringe filters, acidified with pre-prepared 1:1 nitric acid to pH < 2, and stored in a 4 °C incubator for determination of soluble Mn and Fe. Raw water samples were transported directly to the laboratory for total nitrogen and total phosphorus analysis. Sediment samples were collected using a column sampler, divided into 5 cm-thick layers starting from the top 10 cm, and transported to the laboratory in sealed plastic bags. Field observations revealed that the reservoir sediment at sampling points was uniformly black, emitted a fishy odor, exhibited low viscosity, and contained no plant root or leaf debris—indicating a strongly reducing sediment environment. Interstitial water from surface sediment samples was extracted via laboratory centrifugation. Samples were centrifuged at 5000 rpm for 10 min using a low-speed centrifuge (SC-3610, Suzhou Sanlian Instrument Co., Ltd.). The supernatant was filtered through a 0.45 μm microporous membrane, yielding the interstitial water. This liquid was acidified with high-concentration nitric acid prior to analysis. Fe and Mn concentrations in pore water, as well as soluble Fe and Mn in acidified samples filtered through 0.45 μm microporous membranes, were determined using laboratory ICP-OES (Optima 8000 Inductively Coupled Plasma Optical Emission Spectrometer, PerkinElmer).

Total nitrogen in water was determined using alkaline potassium persulfate digestion followed by UV spectrophotometry (T6 New Century, Beijing Puxi General Instrument Co., Ltd.): 10.00 mL of sample was transferred to a 25 mL stoppered ground-glass colorimetric tube, diluted to 10.00 mL with water, then add 5.00 ml of alkaline potassium persulfate solution (weigh 40.0 g of potassium persulfate dissolved in 600 ml of water, weigh 15.0 g of sodium hydroxide dissolved in 300 ml of water. After the sodium hydroxide solution cools to room temperature, combine both solutions and adjust the volume to 1000 ml). Securely plug the tube, wrapping gauze and string tightly around the stopper to prevent ejection. Place the colorimetric tubes in an autoclave. Heat until the pressure relief valve vents steam, then close the valve. Continue heating to 120 °C and start timing. Maintain the temperature between 120 and 124 °C for 30 min. Allow natural cooling, open the valve to release steam, remove the outer lid, and take out the colorimetric tubes. Cool to room temperature, then invert the tubes 2–3 times while holding the stoppers to thoroughly mix the contents. Add 1.0 mL hydrochloric acid solution (1:9 dilution) to each tube, dilute to the 25 mL mark with water, cap, and mix thoroughly. Using a 10 mm quartz cuvette, measure absorbance at wavelengths of 220 nm and 275 nm on a UV spectrophotometer with water as the reference.

Determine the nitrogen content by consulting the standard calibration curve prepared as described above, after correcting for the blank test using potassium nitrate standard solution (0.7218 g/L potassium dihydrogen phosphate).

Total phosphorus was determined using the ammonium molybdate spectrophotometric method: Transfer 25 mL of sample into a stoppered graduated cylinder. Add 4 mL of potassium persulfate (50 g/L) to the sample.
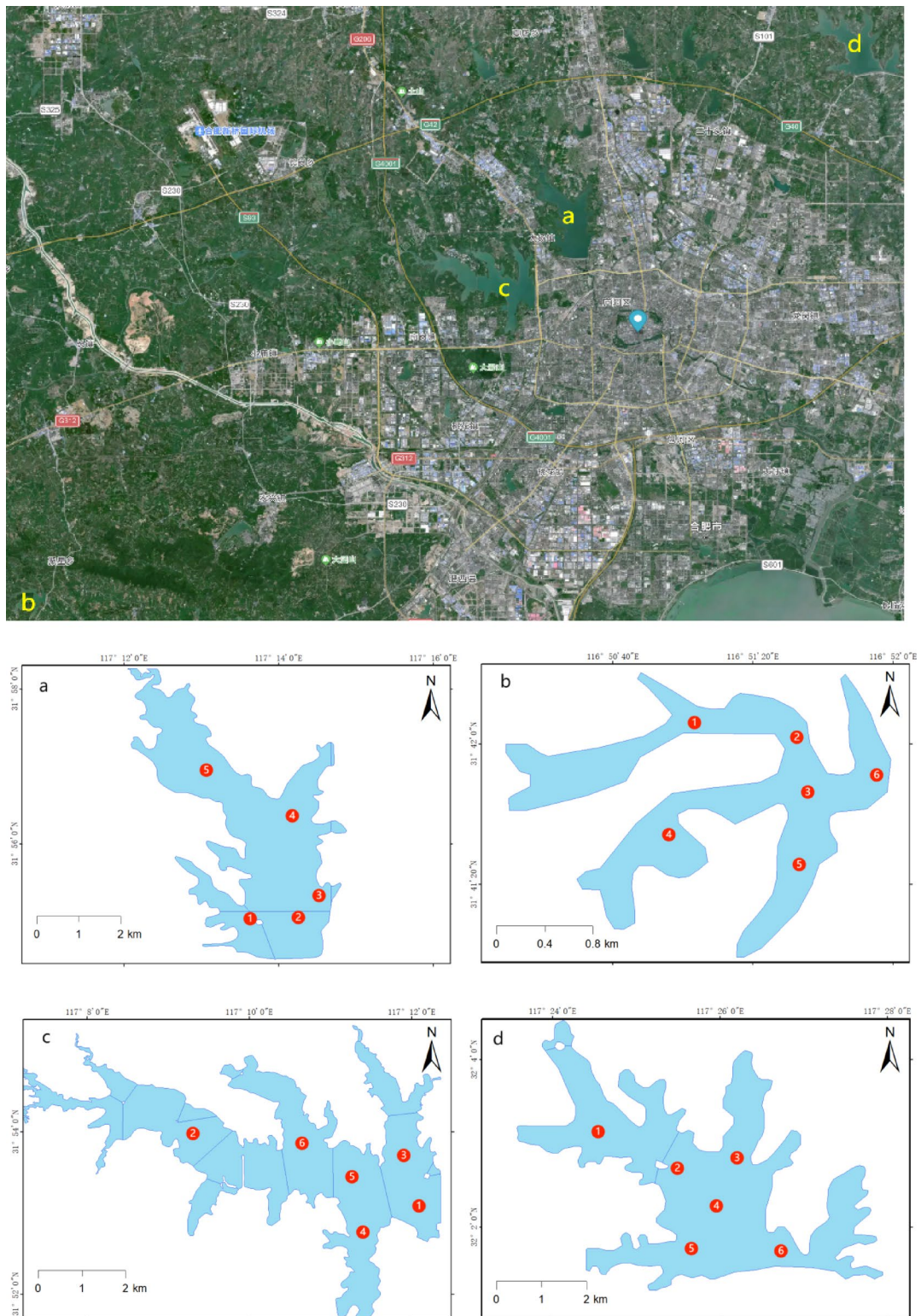
Fig. 1. Reservoir location and sampling point setting (**a**: dafangying, **b**: modun, **c**: dongpu, **d**: zhongxing).

Securely cap the graduated cylinder, then tightly bind the glass stopper with a small cloth and string. Place the cylinder in a large beaker and heat it in an autoclave. Maintain heating at 120 °C (corresponding to 1.1 kg/cm^2 pressure) for 30 min. After the pressure gauge reading drops to zero, remove and cool. Dilute to 50 mL with water. Add 1 mL of ascorbic acid solution (100 g/L) to each digestion solution, shake well, After 30 s, add 2 mL of molybdate solution (prepared by slowly adding 100 mL each of 1.3 g/L ammonium molybdate and 0.035 g/L potassium antimony tartrate to 300 mL concentrated sulfuric acid) and mix thoroughly. Allow to stand at room

Sampling point	Latitude	Longitude
Da 1	117.2277689	31.91628819
Da 2	117.2396565	31.91770885
Da 3	117.2423601	31.92200712
Da 4	117.2369957	31.93726801
Da 5	117.2194004	31.94691858
Mo 1	116.8503285	31.70148052
Mo 2	116.8577957	31.70122493
Mo 3	116.8597269	31.69625912
Mo 4	116.8481827	31.69395869
Mo 5	116.8584824	31.69136607
Mo 6	116.8646193	31.69771968
Dong 1	117.2014618	31.88586623
Dong 2	117.1568298	31.89942072
Dong 3	117.1986294	31.89417406
Dong 4	117.1901321	31.8805459
Dong 5	117.1860981	31.89060324
Dong 6	117.1782017	31.89694317
Zhong 1	117.4089146	32.05108011
Zhong 2	117.4262524	32.04242269
Zhong 3	117.4367237	32.04249545
Zhong 4	117.4323463	32.03420102
Zhong 5	117.4267674	32.02670629
Zhong 6	117.4414444	32.0277978

Table 1. The location of the sample point.

Warm-up time	Decomposition temperature	Hold time
7 min	Room temperature → 120 °C	3 min
5 min	120 °C → 160 °C	3 min
5 min	160 °C → 190 °C	25 min

Table 2. Digestion procedure settings.

temperature for 15 min. Using a 30 mm pathlength cuvette, measure the absorbance at 700 nm with water as the reference. After subtracting the absorbance of the blank test, determine the phosphorus content by consulting the standard calibration curve prepared as described above using a hydrochloride standard solution (0.2197 g/L potassium dihydrogen phosphate, yielding 50 μg/mL phosphorus in the solution) and subtracting the blank test.

Sediment samples collected using a column sampler were divided into 5 cm layers starting from the top 10 cm, placed into sealed plastic bags, and transported to the laboratory. Approximately 50 g of sediment was removed, dried, ground, sieved through a 100-mesh nylon screen, and stored for later use. The dried surface sediment was used for occurrence state analysis, while the remaining samples were analyzed for exchangeable iron and manganese content at different depths. Interstitial water from original surface sediment samples was extracted via laboratory centrifugation. Samples were centrifuged at 5000 rpm for 10 min using a low-speed centrifuge (SC-3610, Suzhou Sanlian Instrument Co., Ltd.). The supernatant was filtered through a 0.45 μm microporous membrane, yielding the interstitial water fraction. Fe and Mn concentrations in the pore water, as well as soluble Fe and Mn in the water body, were determined using laboratory ICP-OES (Optima 8000 Inductively Coupled Plasma Optical Emission Spectrometer, PerkinElmer).

Weigh 0.5 g of air-dried, sieved sample and moisten with a small amount of laboratory water. In a fume hood, sequentially add 6 mL nitric acid, 3 mL hydrochloric acid, and 2 mL hydrofluoric acid to ensure thorough mixing of the sample and digestion solution. Perform digestion using a microwave digestion system (MARS 6, Peian Technology Co., Ltd.) following the heating program in Table 2, then acid-drive using a graphite acid-drive apparatus (GS-5, Seek Great Technology). When the liquid becomes viscous, remove and allow to cool slightly. Rinse the crucible walls with a small amount of nitric acid using a pipette to dissolve residues adhering to the walls using residual heat. Transfer the contents to a 25-mL volumetric flask. Repeat the rinsing procedure with a pipette of nitric acid, combining all rinses into the flask. Dilute to the mark with nitric acid, mix thoroughly, and let stand for 60 min. Transfer the supernatant for ICP-OES analysis to determine Fe and Mn concentrations in the sediment.

Determination of Total Nitrogen in Sediments by Kjeldahl Method: Weigh 0.25 g of air-dried, sieved sample into a Kjeldahl digestion flask. Moisten with a small amount of water (approximately 1 mL), then add 4 mL of

concentrated sulfuric acid. Cover the flask opening with a small funnel and rotate the flask to mix thoroughly. Allow to stand for at least 8 h. Using a dry long-neck funnel, add 0.5 g of sodium thiosulfate pentahydrate reducing agent (ground and sieved to 0.25 mm; prepare fresh for each use) to the bottom of the Kjeldahl digestion flask. Place on an electric hotplate and heat until fumes appear, then cease heating. After cooling, add 1.1 g of catalyst (prepare by thoroughly mixing 200 g potassium sulfate, 6 g copper sulfate pentahydrate, and 6 g titanium dioxide in a glass mortar until finely ground). Shake well and continue digestion on the hot plate. Maintain a gentle boil during digestion, allowing white fumes to reach one-third of the flask neck. When the digestion solution and soil sample turn grayish-white with a slight green tint, digestion is complete. Continue digestion for 1 h, then cool. Transfer the entire digestion solution to a distillation flask. Rinse the Kjeldahl digestion flask 4–5 times with water, using no more than 80 ml total, and connect it to the Kjeldahl distillation apparatus. In a 250-mL conical flask, add 20 mL boric acid solution (20 g/L) and 3 drops of mixed indicator (0.1 g bromocresol green and 0.02 g methyl red dissolved in 100 mL anhydrous ethanol) to absorb the distillate. Ensure the tip of the connecting tube extends below the surface of the absorption solution. Tilt the distillation flask at a 45° angle. Slowly add 20 mL of sodium hydroxide solution (400 g/L) along the flask wall to form an alkaline layer at the bottom. Quickly attach the nitrogen determination bulb and condenser. Shake the flask to thoroughly mix the solution. Begin distillation and stop when approximately 100 mL of distillate has collected. Rinse the end of the condenser with a small amount of water adjusted to pH 4.5. Titrate the distillate with standard hydrochloric acid solution (0.01 mol/L). The solution color changes from blue-green to red–purple. Record the volume of standard hydrochloric acid solution used. Total nitrogen content in the soil is calculated using the following formula:

$$\omega_N = \frac{(V_1 - V_0) \times c_{HCL} \times 14.0 \times 1000}{m \times \omega_{dm}}$$

where: ω_N is the total nitrogen content in the sediment, mg/kg; V_1 is the volume of standard hydrochloric acid solution consumed by the sample, ml; V_0 is the volume of standard hydrochloric acid solution consumed by the blank, ml; c_{HCl} is the concentration of the hydrochloric acid standard solution, mol/L; 14 is the molar mass of nitrogen, g/mol; ω_{dm} is the dry matter content of the soil sample, %; m is the mass of the weighed soil sample, g.

Determination of Total Phosphorus in Sediments by Alkali Fusion-Molybdenum Antimony Colorimetric Method: Weigh 0.25 g of air-dried, sieved sample; moisten the sample with a few drops of anhydrous ethanol; Then add 2 g of sodium hydroxide to evenly cover the sample surface, seal the crucible with its lid; place the crucible in a muffle furnace and heat. When the temperature reaches approximately 400 °C, maintain for 15 min; then continue heating to 640 °C and maintain for another 15 min before removing to cool. Next, add 10 mL of pure water to the crucible and heat to 80 °C. Once the fused residue dissolves, transfer the entire crucible solution into a 50 mL centrifuge tube. Wash the crucible three times with 10 mL portions of sulfuric acid solution (1:4). Transfer the washings to the centrifuge tube. Repeat the rinse with water three more times, transferring each wash to the centrifuge tube. Centrifuge at 2500–3500 r/min for 10 min. After settling, transfer the supernatant to a 100-mL volumetric flask and dilute to the mark with water. Measure 10.0 mL of the test solution into a 50 mL stoppered colorimetric tube and add water to the mark. Add 2–3 drops of 2,4-dinitrophenol indicator (0.02 g/L) to each tube. Adjust the pH to approximately 4.4 using sulfuric acid solution (1:4) and sodium hydroxide solution (2 mol/L) until the solution turns faintly yellow. Subsequent color development and measurement procedures follow the method described for total nitrogen in water.

To ensure experimental accuracy, all reagents used were analytical grade chemicals requiring no further purification. All experimental water was prepared using an ultrapure water system (U-Pure II-200, U-Pure Instruments).

The BCR stepwise extraction method proposed by the European Community Bureau of Standards is an improvement over the Tessier method. This technique can isolate three forms: weakly acid-soluble (e.g., carbonate-bound), reducible (e.g., Fe, Mn-compound-bound), and oxidizable (e.g., organic-bound). Another method is the five-step sequential chemical extraction technique first proposed by Tessier in 1979. This method uses chemical reagents with different solubility capacities to classify the existence forms of heavy metals into: exchangeable phase, carbonate-bound phase, Fe and Mn oxide-bound phase, organic sulfide and sulfide-bound phase, and residual phase. Metals in the residual phase originally existed in primary minerals, termed the primary geochemical phase. The remaining four phases form through weathering of the primary phase, involving exchange adsorption, complexation, precipitation, etc., collectively termed the secondary geochemical phase. A portion of surface sludge was analyzed for occurrence state. The stepwise BCR extraction procedure is detailed in Table 3.

Data analysis
Water correlation analysis
Vertical temperature and dissolved oxygen analysis of reservoirs
As shown in Fig. 2, affected by high summer temperatures, the water bodies in the four reservoirs exhibited distinct thermal stratification in August 2024. Surface water temperatures remained stable around 32 °C. Due to thermal stratification, vertical heat transfer within the water column was impeded, causing water temperatures to decrease gradually with increasing depth. Within the 0–8-m water column, temperature variation was minimal, approximately 3 °C, indicating relatively homogeneous water conditions influenced by the warm surface layer. However, below 8 m, temperature decreased significantly by about 7 °C, forming a distinct thermocline where the temperature gradient between upper and lower layers exceeded 1 °C/m. Under the influence of thermal stratification, dissolved oxygen distribution also undergoes significant changes. Due to the separation between surface and bottom water layers, dissolved oxygen consumption is more intense in the bottom layer. Surface water maintains dissolved oxygen levels between 7.21 and 7.72 mg/L. However, dissolved oxygen content

Steps	Forms of heavy metals	Extractant	Volume/ml	Temperature/°C	Test procedure
1	Commutable State	0.11 mol/L Acetic acid solution	20	22±0.5	Shake continuously for 16 h, then centrifuge at 4000 rpm for 15 min. Remove a portion of the supernatant, filter it (using a 0.45 μm filter membrane, same below), and store it at 4 °C for later testing. Add 20 ml of deionized water to the residue, wash it, and centrifuge for 15 min. Discard the wash solution and retain the residue for use in the next step
2	Oxidizable State	0.1 mol/L hydroxylamine hydrochloride (adjusted to pH 2 using 2 mol/L HNO₃)	20	22±0.5	Shake continuously for 16 h, then centrifuge at 4000 rpm for 15 min. Remove a portion of the supernatant, filter it, and store at 4 °C for later testing. Add 20 mL of deionized water to the residue, wash it, and centrifuge for 15 min. Discard the wash solution and retain the residue for use in Step 3
3	Reduced State	8.8 mol/L H2O2	20	22±0.5	First add 5 mL of 8.8 mol/L H_2O_2, let stand at 25 °C for 1 h, then add another 5 mL of 8.8 mol/L H_2O_2 and incubate in a water bath at 85 °C for 1 h. Add 20 mL of 1 mol/L NH_4OAc and shake at room temperature for 16 h. Centrifuge at 4000 rpm for 15 min. Remove a portion of the supernatant, filter it (using a 0.45 μm filter membrane; same applies below), and store it at 4 °C for later testing. Add 20 mL of deionized water to the residue, wash it, and centrifuge for 15 min. Discard the washing solution; retain the residue for use in Step 4
4	Residual State	HNO3	5	185±0.5	Digest for 8 h. After digestion, dilute the solution to 100 mL in a polyethylene volumetric flask, adjust the volume, and filter a portion of the solution for analysis
		HF	5		
		HClO4	2		

**Table 3**. Step-by-step BCR extraction procedure.
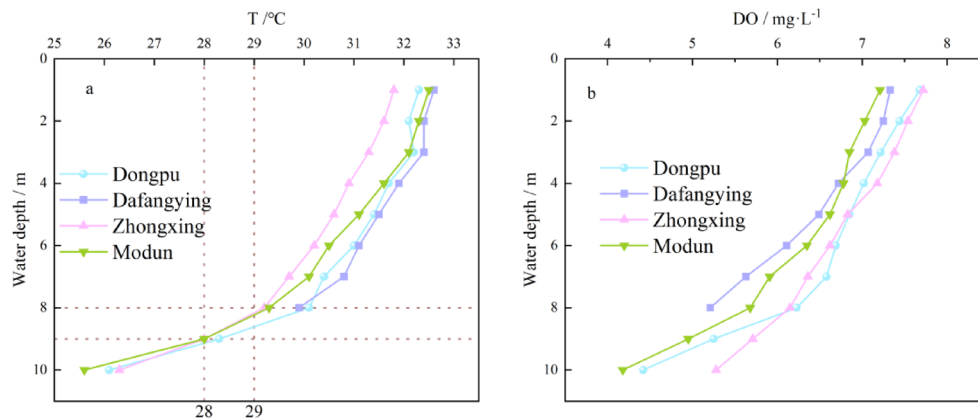
Fig. 2. Vertical variation of water temperature and dissolved oxygen in each section of the reservoir (**a**: water temperature, **b**: dissolved oxygen).

decreases rapidly with increasing depth. Between 0 and 8 m, the concentration gradually declines but relatively smoothly. Below 8 m, dissolved oxygen drops sharply, particularly in Modun Reservoir where bottom-water concentrations reach a minimum of only 4.18 mg/L.

Analysis of total phosphorus indicators in water bodies
As shown in Fig. 3, the total phosphorus content in the water of the four reservoirs exhibits a distinct layered distribution pattern during the summer. Specifically, the total phosphorus concentration in the surface layer is relatively low, around 0.025 mg/L. As the water depth increases, the total phosphorus concentration remains relatively stable at a low level in the 0–6 m depth range. However, as the depth continues to increase, when the depth reaches about 10 m, the total phosphorus concentration rises significantly, reaching its maximum value of approximately 0.15–0.2 mg/L.

Evaluation of reservoir water eutrophication
The hybrid weighted mode method was selected to evaluate eutrophication in the study area's reservoirs, using TN and TP as assessment indicators. Results were expressed as the eutrophication evaluation composite index (PI). Compared to the simple superposition method, vector analysis method, and square root of sum of squares method, this approach offers superior resolution and greater reliability. The calculation formula for this method is:

$$I_i = \frac{C_i}{C_{i0}}$$
$$PI = \sum\nolimits_1 W_{i1} I_i + \sum\nolimits_2 W_{i2} I_i$$
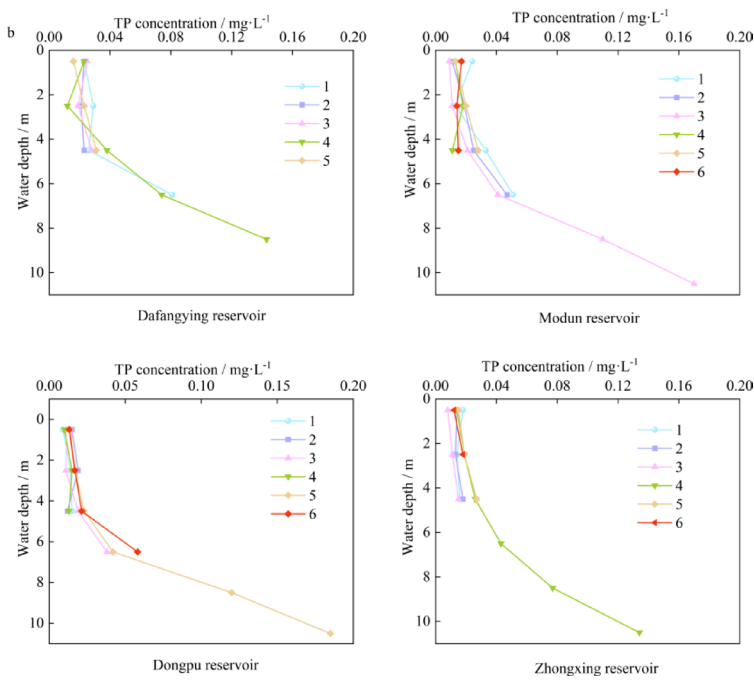
Fig. 3. Vertical variation of total phosphorus in each section of the reservoir.

Degree of eutrophication	Level of eutrophication	PI value
Not eutrophic	I	PI<0.2
Lightly enriched	II	$0.2 \leq PI < 1$
Moderately nutrient-rich mesotrophic	III	$1 \leq PI < 5$
Heavy nutrient enrichment	IV	$5 \leq PI < 10$
Severe eutrophication	V	$PI \geq 10$

Table 4. Evaluation standard for eutrophication of reservoirs.

Reservoirs	PI value	Level of eutrophication
Dafangying	0.35	II
Modun	0.75	II
Dongpu	0.68	II
Zhongxing	0.41	II

Table 5. Eutrophication assessment form.

In the formula: I_i is the sub-index; C_i is the measured value representing the pollutant; C_{i0} is the standard value corresponding to the pollutant. For the reservoir water quality standards in the study area, calculated based on Class II surface water standards: TN = 0.5 mg/L and TN = 0.1 mg/L; P_I is the comprehensive index for eutrophication assessment; Σ_1 is the sum over all i where i > 1; Σ_2 is the sum over all i; where $\Sigma_1 W_{i1} = 1$ and $\Sigma_2 W_{i2} = 1$. W_{i1} and W_{i2} constitute the weighting coefficients. The calculation results are used to classify the reservoir's eutrophication level according to the Reservoir and Lake Nutrient Classification Standards (Table 4). The grading results are shown in Table 5.

Analysis of soluble Fe and Mn in water bodies
As shown in Fig. 4, the soluble Fe and Mn concentrations in the surface water layer are both below the limit values specified in the National Class II Safe Drinking Water Standard (Mn < 0.1 mg/L, Fe < 0.3 mg/L, GB5749). Specifically, the Fe concentration is less than 0.05 mg/L and the Mn concentration is less than 0.1 mg/L, indicating that the Fe and Mn levels in the surface water meet safe drinking water standards. However, soluble Fe and Mn concentrations gradually increase with depth. Under thermal stratification, limited exchange between surface and bottom waters leads to accumulation of Fe and Mn in the lower zones. Near the bottom layer,
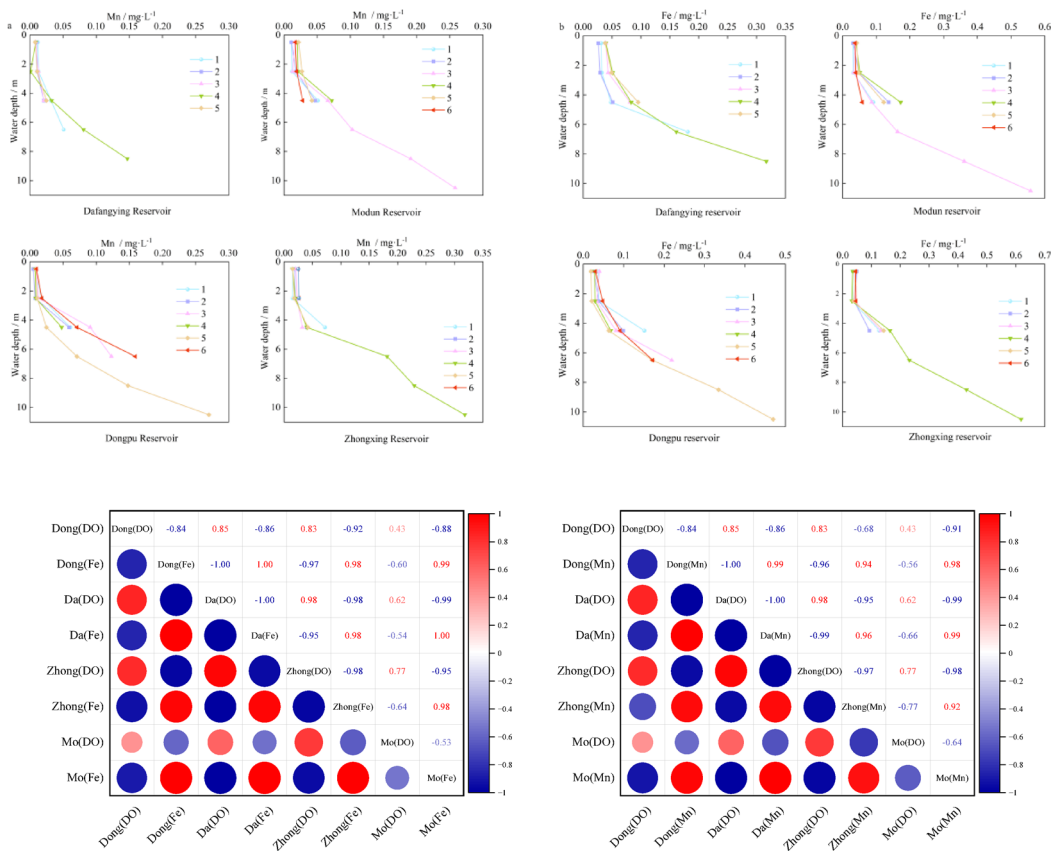
Fig. 4. Vertical variation diagram of soluble iron and manganese in each section of the reservoir (**a**: soluble manganese, **b**: soluble iron).
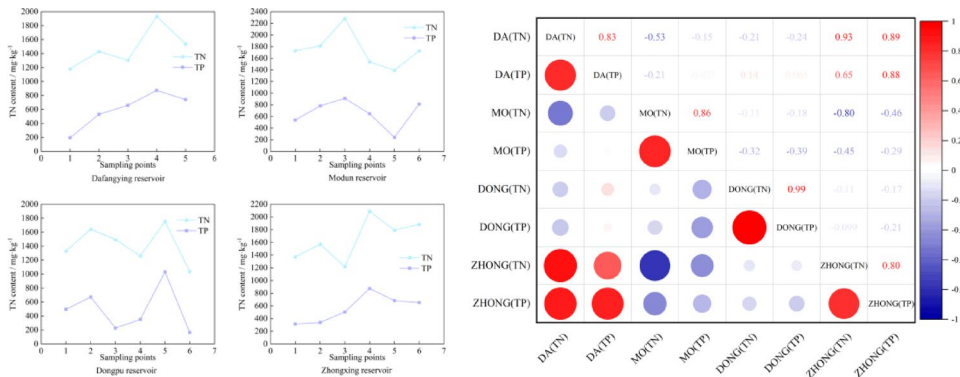
Fig. 5. Total nitrogen and total phosphorus content of surface sediments.

soluble Fe and Mn concentrations markedly increased, exceeding safety standards to reach 0.30–0.70 mg/L and 0.15–0.30 mg/L, respectively, indicating both elements surpassed permissible limits.

Characteristics of endogenous pollution in sediment–water environments

Analysis of nitrogen and phosphorus nutrient content in surface sediments

As shown in Fig. 5, the total nitrogen (TN) and total phosphorus (TP) content in the reservoir's surface sediments exhibited significant fluctuations. The TN content in the surface sediments ranged from 1036.28 to 2282.12 mg/kg, while the TP content fluctuated between 164.32 and 1032.17 mg/kg. The variation trends of TN and TP at each sampling point showed certain similarities, with maximum values typically occurring at the deepest water depths. Furthermore, TN and TP exhibited a highly significant positive correlation (Pearson correlation coefficient $r > 0.80$, $p < 0.01$), indicating that their accumulation in reservoir sediments is closely related.
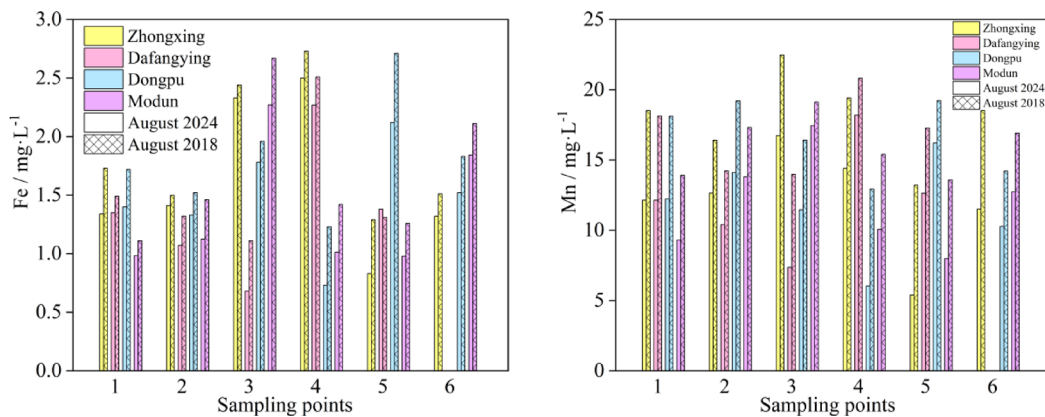
Fig. 6. Iron and manganese content of interstitial water in surface sediments.
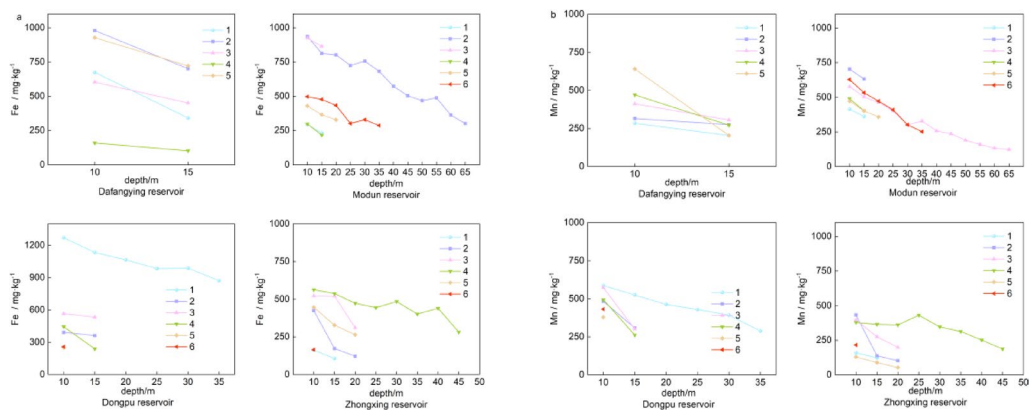
Fig. 7. Vertical distribution of iron and manganese in reservoir sediments (**a**: commutable iron, **b**: commutable manganese).

Analysis of Fe and Mn content in interstitial water of surface sedime
As shown in Fig. 6, in August 2024, the concentrations of Fe and Mn in the interstitial water of surface sediments in the drinking water reservoir of Hefei City during the wet season ranged from 0.68 to 2.33 mg/L for Fe and from 5.39 to 18.19 mg/L for Mn. At greater water depths, the concentrations of Fe and Mn were generally higher. Further comparative analysis reveals that the concentrations of Fe and Mn in August 2024 were lower than those in the interstitial water of surface sediments in the reservoir in August 2018. Specifically, the concentrations of Fe and Mn have decreased over the eight years, suggesting a possible trend of ecological improvement in the reservoir or a gradual effectiveness of water management measures.

Vertical distribution of Fe and Mn in sediments
Figure 7 shows the vertical distribution of Fe and Mn in sediments at different sampling points. According to the analysis of Fig. 7, the total amount of Fe and Mn in the sediments of each reservoir generally shows that Fe content is higher than Mn content. In all four reservoirs, the vertical distribution characteristics of Fe and Mn are highly similar, with the highest concentrations observed in the surface layer, which gradually decrease with increasing depth. Notably, in the Zhongxing and Modun reservoirs, the Fe and Mn concentrations in the surface sediments reached their maximum values at deeper sampling points, at 1940 mg/kg and 1049.2 mg/kg, respectively.

Distribution characteristics of sediment forms and ecological risk assessment
Distribution characteristics of Fe and Mn forms in surface sediments
The analysis results are shown in Fig. 8. In the sediments, Fe mainly exists in the residual form, accounting for more than 70% in most cases. Additionally, the reducible Fe content in the sediments is relatively high, ranging from 2229.5 to 10,850 mg/kg, with a significant variation in concentration. In the Mn form distribution at different sampling points, the highest proportion is found in the exchangeable Mn form, ranging from 284 to 640.5 mg/kg, indicating that Mn predominantly exists in the exchangeable form in the sediments. Comparing the Mn form analysis results with those from the other four reservoirs, only in the surface sediments of the
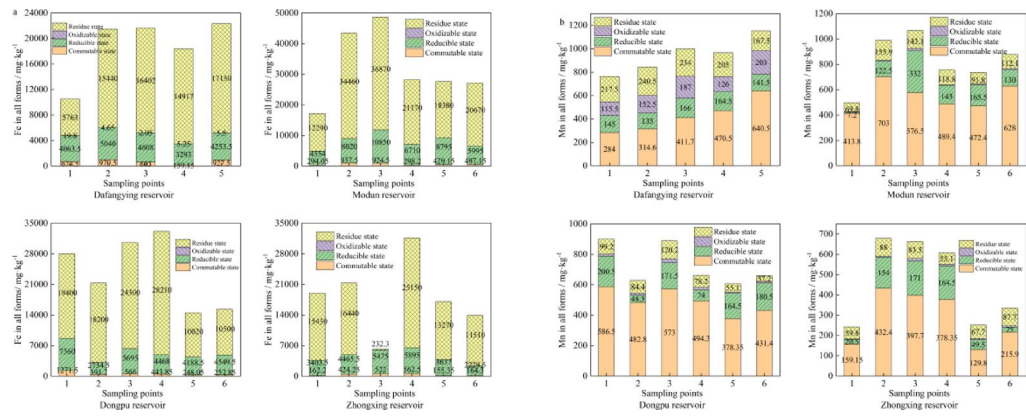
Fig. 8. Morphological distribution of iron and manganese in sediments (**a**: iron, **b**: manganese).

I_{geo}	<0	0–1	1–2	2–3	3–4	4–5	>5
Pollution level	I	II	III	IV	V	VI	VII
Degree of pollution	None	Light pollution	Light to moderate pollution	moderate pollution	Light to moderate pollution	Severe pollution	Serious pollution

Table 6. Accumulation index and pollution grading standards.

Dafangying Reservoir was a small amount of oxidizable Mn detected, with concentrations ranging from 115.5 to 203 mg/kg.

Risk analysis using the cumulative index method
The Cumulative Index Method (I_{geo}) proposed by Muller from Heidelberg University, Germany, is used here. It is a quantitative indicator for studying the concentration of heavy metals in sediments and was used to assess the Fe and Mn content in the sediments of the reservoirs. The calculation formula is as follows:

$$I_{geo} = log_2[C_n / (k \times B_n]$$

In the formula: B_n: the geochemical background value of element n in the sediment; C_n: the measured concentration of heavy metal element n in the sediment; k: the constant that accounts for fluctuations in the sedimentary background value, typically taken as $k = 1.5$.

Based on the I_{geo} values, the degree of heavy metal pollution is classified according to the standards in Table 6. In this study, the Fe and Mn content in the shoreline soils of various reservoirs (including the Dafangying No. 2, Modun No. 4, Dongpu No. 4, and Zhongxing No. 5 sampling points) were selected as the geochemical background values for evaluating Fe and Mn pollution in the surface sediments. The results of the heavy metal I_{geo} and the index classification are shown in Table 7.

Discussion
Summer thermal stratification in reservoirs refers to temperature differences formed by factors such as solar radiation and air temperature variations, typically manifesting across different depths within the reservoir. Due to higher summer temperatures, surface water warms while bottom water cools rapidly, creating a thermal stratification phenomenon. This stratification impedes vertical material circulation in the water body, leading to vertical variations in dissolved oxygen, nutrients, and other components. Furthermore, thermal stratification creates anoxic/anaerobic conditions in the bottom layer, promoting the release of endogenous pollutants like iron (Fe), manganese (Mn), and phosphorus from sediments into the water column. The presence of thermal stratification alters the vertical distribution of parameters such as dissolved oxygen, pH, Fe, and Mn within reservoir waters. However, the intrinsic mechanisms governing thermal stratification formation and its influencing factors require further investigation to achieve a more comprehensive understanding.

Comparing Fig. 1 reveals that vertical changes in water temperature directly influence the vertical distribution of dissolved oxygen. Higher dissolved oxygen levels in surface waters primarily result from atmospheric reoxygenation. At this stage, water depths are shallow, and no thermocline has formed. Dissolved oxygen in the surface layer can thus migrate downward, ensuring relatively consistent dissolved oxygen levels throughout the shallow water column. However, when water depth reaches 8 m, a thermocline forms, dividing the water column into upper and lower layers. Below the thermocline, dissolved oxygen cannot migrate downward. Simultaneously, microorganisms in the bottom sediment continuously consume dissolved oxygen while decomposing organic matter, leading to reduced dissolved oxygen levels in the bottom water layer. Processes such as the respiration of benthic organisms, the mineralization of organic matter in sediments, and the aerobic degradation by microorganisms further accelerate the consumption of dissolved oxygen at the bottom. The

Sampling point	Mn	Fe
Da 1	−0.07/ Ⅰ	−0.61/ Ⅰ
Da 2	−0.58/ Ⅰ	−0.58/ Ⅰ
Da 3	0.35/ Ⅱ	−0.92/ Ⅰ
Da 4	0.48/ Ⅱ	−0.59/ Ⅰ
Da 5	0.38/ Ⅱ	0.01/ Ⅱ
Mo 1	−0.58/ Ⅰ	−1.00/ Ⅰ
Mo 2	−0.50/ Ⅰ	−0.58/ Ⅰ
Mo 3	0.25/ Ⅱ	−0.22/ Ⅰ
Mo 4	−1.78/ Ⅰ	−0.57/ Ⅰ
Mo 5	−0.34/ Ⅰ	−1.33/ Ⅰ
Mo 6	−0.43/ Ⅰ	−0.65/ Ⅰ
Dong 1	−0.08/ Ⅰ	0.16/ Ⅱ
Dong 2	−0.36/ Ⅰ	−0.40/ Ⅰ
Dong 3	−0.16/ Ⅰ	−0.41/ Ⅰ
Dong 4	−0.58/ Ⅰ	−0.58/ Ⅰ
Dong 5	0.13/ Ⅱ	0.21/ Ⅱ
Dong 6	0.04/ Ⅱ	−0.26/ Ⅰ
Zhong 1	0.13/ Ⅱ	0.10/ Ⅱ
Zhong 2	−0.59/ Ⅰ	0.15/ Ⅱ
Zhong 3	−0.21/ Ⅰ	0.31/ Ⅱ
Zhong 4	0.81/ Ⅰ	−0.31/ Ⅰ
Zhong 5	−0.58/ Ⅰ	−0.58/ Ⅰ
Zhong 6	0.16/ Ⅱ	−0.63/ Ⅰ

Table 7. The geoaccumulation index and classification grade of Fe and Mn in sediments at different sampling sites.

continuous depletion of DO in the bottom layer leads to anoxic or even anaerobic conditions, releasing reductive substances like phosphorus, ammonium, Mn^{2+}, and Fe^{2+}[17]. When thermal stratification in the reservoir dissipates, these substances mix with the surface water, exacerbating eutrophication. Therefore, bottom DO concentrations in reservoirs can also reflect their trophic status to a certain extent[18]. This finding is consistent with studies conducted at Panjiakou Reservoir and the Pearl River Estuary[19,20].

In the surface waters of reservoirs, algae growth is typically vigorous due to strong sunlight and water flow, with photosynthesis helping to reduce total phosphorus concentrations. Deeper water layers are generally rich in organic matter, have lower dissolved oxygen concentrations, and exhibit relatively uniform flow without significant stratification or water exchange, resulting in minimal fluctuations in total phosphorus levels. However, the formation of thermoclines creates anoxic conditions in the bottom layer, further promoting phosphorus release from sediments into the water. This results in elevated total phosphorus concentrations in the bottom layer, with phosphorus levels in the bottom waters of four drinking water reservoirs in Hefei exceeding Class II water quality standards[21]. Nutrient enrichment assessments using the mixed-weighted model revealed that all four reservoirs exhibited PI (Comprehensive Nutrient Enrichment Index) values below 1 during August, indicating low nutrient enrichment. This assessment holds significant implications for water quality safety.

As previously mentioned, the primary cause of excessive Fe and Mn concentrations is thermal stratification, which depletes dissolved oxygen at the bottom. Thermal stratification is extremely common in deep-water reservoirs. Bottom Fe and Mn concentrations exhibit a negative correlation with dissolved oxygen levels, with soluble Fe and Mn concentrations generally higher in bottom waters where dissolved oxygen is low. This phenomenon aligns with the geochemical theory predicting the reduction and dissolution of iron and manganese. Iron and manganese are essential trace elements for organisms. The primary issues arising from their massive release in anoxic conditions center on water quality deterioration. During reoxidation, Fe^{2+} and Mn^{2+} form colored colloidal substances, leading to "black water" or "yellow water" phenomena and producing unpleasant odors. This severely impacts the sensory characteristics of water sources while significantly increasing the difficulty and cost of water treatment processes. Furthermore, the ecological risks of iron and manganese release manifest more as indirect effects: the reductive dissolution of iron oxides disrupts the adsorption equilibrium of phosphorus at the sediment–water interface, leading to the synergistic release of endogenous phosphorus from sediments. This exacerbates water eutrophication, potentially triggering algal blooms and posing indirect threats to aquatic ecosystems.

Thermal stratification causes oxygen depletion in bottom water, leading to extensive reduction of Fe and Mn in sediments under anoxic conditions, which then diffuse upward into overlying water. As depth increases, Fe and Mn concentrations gradually rise, leading to exceedances of regulatory limits. Therefore, the primary cause of seasonal fluctuations in Fe and Mn concentrations in Hefei reservoirs during summer is thermal stratification. This stratification reduces dissolved oxygen levels in bottom waters, allowing microbial activity to reduce Fe and

Mn within sediments and release them into the water column, resulting in excessive Fe and Mn concentrations in the bottom water layer.

Nutrients such as nitrogen and phosphorus in lake and reservoir sediments are key contributors to eutrophication and significantly influence biological productivity and sediment fertility. Beyond environmental factors like pH and dissolved oxygen (DO), sediment pollution release is also affected by microbial metabolic activities within the sediments[22]. For instance, prokaryotic microorganisms, including phototrophic and heterotrophic types, can alter environmental conditions through assimilation, dissimilation, and secretion of metabolic products, thereby influencing the transformation and fate of nutrients in sediments[9]. Analyses reveal a significant positive correlation between total nitrogen and total phosphorus, indicating a clear association between the sources of nitrogen and phosphorus in sediments and their migration and transformation in water. Research indicates that total nitrogen and phosphorus in sediments primarily originate from endogenous biological decomposition, a process accompanied by substantial nitrogen and phosphorus release that may severely pollute water quality. Not all nitrogen and phosphorus in sediments are directly released into overlying water; only relatively "active" forms undergo transformation and migration at the sediment–water interface[23,24].

A comparison of the concentrations of Fe and Mn in the interstitial water of surface sediments and the overlying water reveals that the concentrations of Fe and Mn in the interstitial water are tens to even hundreds of times higher than in the overlying water. Since there is no external source of Mn input around the reservoir, it indicates that the Fe and Mn in the sediments do not directly enter the overlying water. Instead, they diffuse upward through the concentration gradient via interstitial water and are influenced by the re-sedimentation process at the sediment–water interface.

Comparing Fe and Mn concentrations in pore water of surface sediments with those in the overlying water column reveals that Fe and Mn concentrations in pore water are tens to hundreds of times higher than in the overlying water. Given the absence of external Fe and Mn inputs around the reservoir, this indicates that Fe and Mn in sediments do not directly enter the overlying water. Instead, they diffuse upward through pore water via concentration gradients, influenced by resuspension at the sediment–water interface. Analysis of Fe concentration variations revealed that summer heat and bottom water hypoxia promote organic matter mineralization, leading to Fe reduction and release into pore water. Intense bacterial activity during summer can reduce solid Fe to liquid Fe. Studies indicate that dissolved oxygen (DO) levels influence the redox environment of water bodies[25]. The anaerobic conditions in the reservoir's bottom layer during thermal stratification periods lower the redox potential at the water–sediment interface[26,27]. Mn possesses a higher redox potential than Fe, making its release more readily achievable. Consequently, under aerobic conditions, Fe and Mn concentrations at the sediment–water interface typically exhibit a distribution pattern characterized by lower concentrations in pore water and higher concentrations within sediments. Low-concentration surface pore water and metal oxide layers effectively inhibit the further release of other dissolved pollutants, such as phosphates, into the water body. It is important to note that the decrease in Fe and Mn concentrations in sediment pore water may reflect the impact of reservoir water quality changes on the release and adsorption behavior of metallic elements. As water quality improves, harmful substances within sediments may gradually become immobilized or transformed into harmless forms, thereby reducing dissolved Fe and Mn levels in the water body. This change has positive implications for reservoir water quality, ecosystem stability, and drinking water safety.

During summer, peak concentrations of Fe occur in sediment pore water, mirroring the distribution patterns of Fe within sediments and both being linked to the redox conditions within the sediment matrix. Internally, reducing conditions trigger the release of substantial dissolved Fe, which then migrates upward along concentration gradients. However, due to the anaerobic conditions at the surface layer, dissolved Fe cannot oxidize and precipitate there; instead, it is released upward into the overlying water. Fe primarily exists as residual form, indicating its reluctance to release and environmental harmlessness. Exchangeable Mn constitutes the largest proportion, suggesting the surface sediment readily undergoes exchange reactions with external metal cations, releasing Mn and consequently elevating Mn levels in the reservoir. The presence of oxidizable Mn in the surface sediments of Dafangying Reservoir may explain its higher redox potential compared to other reservoirs. This oxidizable Mn exists as mineral envelopes and finely dispersed particles with large surface areas, enabling adsorption or complexation with co-precipitated anions.

The vertical distribution of Fe and Mn shows decreasing concentrations with increasing depth, indicating that the surface layer of sediments may be subject to stronger oxidation or higher biological activity. This leads to the enrichment of Fe and Mn in the surface layer, with Fe and Mn in the sediments primarily originating from the cumulative precipitation of Fe and Mn minerals in the geological environment[28,29].

Based on measured heavy metal concentrations and calculated biogeochemical accumulation indices, only Dafangying and Zhongxing reservoirs showed mild contamination, with all others classified as uncontaminated. This discrepancy likely stems from runoff pollution—where rainfall carries substantial pollutants into reservoirs—leading to Mn contamination exceeding standards in bottom sediments.

Conclusions

This study systematically investigated and analyzed iron and manganese in water and sediments of typical reservoirs in the Jianghuai region, revealing significant vertical spatial differentiation. Results indicate that the stable thermal stratification formed during summer is the key physical driver controlling iron-manganese geochemical behavior. Thermal stratification induces seasonal anoxic (and even anaerobic) conditions in the bottom water layer, promoting the reduction and dissolution of iron-manganese oxides in sediments. This leads to significant enrichment of Fe and Mn in the bottom water and at the sediment–water interface. Notably, manganese release precedes iron, making its concentration changes a sensitive "early warning indicator" for shifts in the bottom redox environment. Comprehensive evaluation of eutrophication status indicates that reservoirs in this region generally exhibit low eutrophication levels with overall good water quality. However,

summer vertical water column profiling data reveal a marked increase in iron and manganese concentrations from surface to bottom layers, with bottom-layer concentrations reaching tens of times higher than surface levels. This phenomenon clearly demonstrates that despite the overall low nutrient status, significant risks of endogenous iron and manganese release persist throughout the reservoir, posing a potential threat to drinking water source quality. Further investigation into the release patterns and fluxes of iron and manganese in sediments is crucial for safeguarding drinking water sources in the Jianghuai region. This study elucidates the endogenous release mechanism driven by thermal stratification, shifting water quality risk monitoring from end-point concentration surveillance to monitoring physical structures (thermal stratification) and early chemical indicators. This provides scientific basis for precise prevention, control, and safety management of regional reservoir water quality.

Data availability

The datasets used and/or analyzed during the current study are available from the corresponding author on reasonable request.

References

1. Xu, J. et al. The influence of pollutant sources and water stratification on water quality in Lijiahe Reservoir. *Environ. Sci.* **40**, 3049–3057 (2019).
2. Zhang, Y. et al. Dissolved oxygen stratification and response to thermal structure and long-term climate change in a large and deep subtropical reservoir (Lake Qiandaohu, China). *Water Res.* **75**, 249–258 (2015).
3. Krueger, K. M. et al. Iron and manganese fluxes across the sediment-water interface in a drinking water reservoir. *Water Res.* **182**, 116003 (2020).
4. Micić, V. Variations of common riverine contaminants in reservoir sediments. *Sci. Total Environ.* (2013).
5. Barbieri, M., Sappa, G., Vitale, S., Parisse, B. & Battistel, M. Soil control of trace metals concentrations in landfills: A case study of the largest landfill in Europe, Malagrotta, Rome. *J. Geochem. Explor.* (2014).
6. Sundaray, S. K., Nayak, B. B., Lin, S. & Bhatta, D. Geochemical speciation and risk assessment of heavy metals in the river estuarine sediments—A case study: Mahanadi basin, India. *J. Hazard. Mater.* **186**, 1837–1846 (2011).
7. Zhang, J. Assessment of heavy metal pollution and water quality characteristics of the reservoir control reaches in the middle Han River, China. *Sci. Total Environ.* (2021).
8. Huang, L., Fang, H. & Reible, D. Mathematical model for interactions and transport of phosphorus and sediment in the Three Gorges Reservoir. *Water Res.* **85**, 393–403 (2015).
9. Wu, L. Microbial communities in eutrophication of Taihu Lake sediments and their responses to environmental factors. *Chin. J. App. Environ. Biol.* **25**, 1470–1476 (2019).
10. Duan, T., Feng, J., Chang, X. & Li, Y. Evaluation of the effectiveness and effects of long-term ecological restoration on watershed water quality dynamics in two eutrophic river catchments in Lake Chaohu Basin, China. *Ecol. Indicators* **145**, 109592 (2022).
11. Fan, Y.-Y. Mediation of functional gene and bacterial community profiles in the sediments of eutrophic Chaohu Lake by total nitrogen and season. *Environ. Pollut.* (2019).
12. Jetoo, S. Barriers to Effective Eutrophication Governance: A Comparison of the Baltic Sea and North American Great Lakes (2018).
13. Wilson, R. S., Schlea, D. A., Boles, C. M. W. & Redder, T. M. Using models of farmer behavior to inform eutrophication policy in the Great Lakes. *Water Res.* **139**, 38–46 (2018).
14. Reddy, K. R., Fisher, M. M. & Ivanoff, D. Resuspension and diffusive flux of nitrogen and phosphorus in a hypereutrophic lake. *J. Environ. Qual.* **25**, 363–371 (1996).
15. Schwefel, R. et al. Using small-scale measurements to estimate hypolimnetic oxygen depletion in a deep lake. *Limnol. Oceanogr.* **63**, S54–S67 (2018).
16. Ma, X. Manganese ion monitoring and analysis of drinking water sources in Dafangying Reservoir and its pollution mechanism (2016).
17. Jaiswal, D. & Pandey, J. Anthropogenically enhanced sediment oxygen demand creates mosaic of oxygen deficient zones in the Ganga River: Implications for river health. *Ecotoxicol. Environ. Saf.* **171**, 709–720 (2019).
18. Conley, D. J., Carstensen, J., Vaquer-Sunyer, R. & Duarte, C. M. Ecosystem thresholds with hypoxia (2009).
19. Wilhelm, S. & Adrian, R. Impact of summer warming on the thermal characteristics of a polymictic lake and consequences for oxygen, nutrients and phytoplankton. *Freshw. Biol.* (2007).
20. Zhao, Y. et al. Dynamics of inorganic carbon and pH in a large subtropical continental shelf system: Interaction between eutrophication, hypoxia, and ocean acidification. *Limnol. Oceanogr.* **65**, 1359–1379 (2020).
21. GB 3838-2002. Environmental Quality Standards for Surface Water.
22. Huang, H. et al. New insights into odor release from sediments in Lake Chaohu and the potential role of sediment microbial communities. *J. Hazard. Mater.* **491**, 138007 (2025).
23. Kang, M., Peng, S., Tian, Y. & Zhang, H. Effects of dissolved oxygen and nutrient loading on phosphorus fluxes at the sediment–water interface in the Hai River Estuary, China. *Mar. Pollut. Bull.* **130**, 132–139 (2018).
24. Zhao, H. Features and influencing factors of nitrogen and phosphorus diffusive fluxes at the sediment-water interface of Erhai Lake. *Environ. Sci. Pollut. Res.* (2018).
25. Wang, Z., Deng, H., Chen, L., Xiao, Y. & Zhao, F. In situ measurements of dissolved oxygen, pH and redox potential of biocathode microenvironments using microelectrodes. *Biores. Technol.* **132**, 387–390 (2013).
26. Tasnim, B., Jamily, J. A., Fang, X., Zhou, Y. & Hayworth, J. S. Simulating diurnal variations of water temperature and dissolved oxygen in shallow Minnesota lakes (2021).
27. Ya, Z. et al. Effects of the disappearance of seasonal thermal stratification on the mobilization of iron and phosphorus in reservoirs, southern China—A case of Tianbao Reservoir, Nanning City. *J. Lake Sci.* **33**, 1153–1162 (2021).
28. Esmaeilzadeh, M. Origin and comprehensive risk assessment of heavy metals in surface sediments along the Caspian Sea. *Mar. Pollut. Bull.* (2024).
29. Liu, S., Zheng, C., Yuan, Q., Wang, X. & Wang, Z. Characteristics of ferromanganese mass concentration in Changtan Reservoir, Taizhou and its genesis. *Environ. Sci.* **35**, 3702–3708 (2014).

Acknowledgements

Author contributions

Xianhuai Huang is the corresponding author and is responsible for the planning and guidance of the overall research, the final revision and editing of the paper. Kun Wang responsible for research design, data collection, experimental implementation, data analysis, and writing the first draft of the paper. Wei Chen responsible for literature review and background research, participate in data analysis and revision of papers. Yuchao Tang and Beiping Zhang participate in the design and implementation of experiments and provide advice on data analysis methods. Haixiang Sun, Changnian Wu and Jian Huang responsible for research funding applications and project management.

Funding

Declarations

Competing interests

The authors declare no competing interests.

Additional information

Correspondence and requests for materials should be addressed to X.H.

Reprints and permissions information is available at www.nature.com/reprints.

Publisher's note Springer Nature remains neutral with regard to jurisdictional claims in published maps and institutional affiliations.